

Coherent energy scale revealed by ultrafast dynamics of UX_3 (X=Al, Sn, Ga) single crystals

Saritha K. Nair,¹ J.-X. Zhu,² J. L. Sarrao,² A. J. Taylor,² and Elbert E. M. Chia¹

¹*Division of Physics and Applied Physics, School of Physical and Mathematical Sciences, Nanyang Technological University, Singapore 637371, Singapore*

²*Los Alamos National Laboratory, Los Alamos, New Mexico 87545, USA*

(Dated: June 14, 2021)

Temperature dependence of relaxation dynamics of UX_3 (X = Al, Ga, Sn) compounds is studied using time resolved pump-probe technique in the reflectance geometry. UGa_3 is an itinerant anti-ferromagnet, while UAl_3 and USn_3 are spin fluctuation systems. For UGa_3 , our data are consistent with the formation of a spin density wave SDW gap as evidenced from the quasidivergence of the relaxation time τ near the Néel temperature T_N . For UAl_3 and USn_3 , the relaxation dynamics shows a change from single exponential to two exponential behavior below a particular temperature, suggestive of coherence formation of the $5f$ electrons with the conduction band electrons. This particular temperature can be attributed to the spin fluctuation temperature T_{sf} , a measure of the strength of Kondo coherence. Our T_{sf} is consistent with other data such as resistivity and susceptibility measurements. The temperature dependence of the relaxation amplitude and time of UAl_3 and USn_3 were also fitted by the Rothwarf-Taylor model. Our results show ultrafast optical spectroscopy is sensitive to c - f Kondo hybridization in the f -electron systems.

I. INTRODUCTION

The uranium compounds UX_3 , where X is a IIIb (Al, Ga, In, Tl) or IVb (Si, Ge, Sn, Pb) element, crystallize in the cubic $AuCu_3$ -type structure¹ and have U-U distances (d_{U-U}) much larger than the Hill limit (~ 3.5 Å) for uranium compounds.² The different degree of hybridization of the $5f$ electron orbitals with the conduction electron orbitals in these compounds leads to a wide range of magnetic behavior such as Pauli enhanced paramagnetism (UAl_3 , USi_3 , and UGe_3), antiferromagnetism (UGa_3 , UPb_3 and UIn_3), and heavy fermion behavior (USn_3).^{1,3,4} Due to the the above-mentioned properties and the availability of high quality crystals, UX_3 compounds are ideal candidates for studying how physical properties and underlying electronic structure are related.

The anomalous behavior of the resistivities of UX_3 compounds can be explained on the basis of spin fluctuations in narrow $5f$ bands.^{5,6} A temperature characteristic of the spin fluctuations in the UX_3 compounds is the spin fluctuation temperature, T_{sf} , which expresses the strength of hybridization between f and conduction electrons (c - f hybridization). The degree of hybridization is related to the degree of delocalization of the f -electrons. A high value of T_{sf} corresponds to more easily hybridized (delocalized) electrons. Above T_{sf} , f -electrons are localized; whereas below T_{sf} , there is quasiparticle coherence from the hybridization between f -electrons and conduction electrons, *i.e.*, f -electrons now become more delocalized (or itinerant). The effective hybridization below T_{sf} leads to changes in measured physical properties. For example, the electrical resistivity changes from a T -linear law above T_{sf} to a T -quadratic law below this temperature.⁶⁻⁹ The temperature at which the magnetic susceptibility reaches a Curie-Weiss law is theoretically

of the order of T_{sf} .⁶ A modified Curie-Weiss law, *i.e.* $\chi(T) = \chi_0 + C/(T + T^*)$, associates T^* with T_{sf} for relatively strong c - f hybridization.^{10,11}

Ultrafast time-resolved pump-probe spectroscopy has been recognized as a powerful technique to study the nonequilibrium carrier dynamics in strongly correlated electron materials. In addition to distinguishing different phases in a material by their different relaxation dynamics, it can discern whether one phase coexists or competes with another phase in close proximity,^{12,13} giving information on the nature of low energy electronic structure of correlated electron systems, for example, in high-temperature superconductors. Pump-probe experiments have also been performed on actinide compounds, such as the itinerant antiferromagnets $UNiGa_5$ and $UPtGa_5$,^{14,15} and the heavy-fermion superconductor $PuCoGa_5$.¹⁶

The hybridization between the conduction electrons and the localized f electrons also causes a narrow gap to form in the density of states near the Fermi level.¹⁷ This gap, called the hybridization gap, results in a relaxation bottleneck, evidenced by an increase in the relaxation time τ at low temperatures. For example, in heavy fermions such as $YbAgCu_4$ and SmB_6 , τ increases monotonically with decreasing temperature.¹⁷ The temperature dependence of the relaxation amplitude and time were fit using the Rothwarf-Taylor (RT) model. In this paper, we investigate the ultrafast dynamics in three isostructural uranium compounds, UAl_3 , UGa_3 and USn_3 , using the ultrafast pump-probe technique. The variation in hybridization strength is responsible for the differences in properties of these three isostructural compounds. UAl_3 and USn_3 are categorized as spin-fluctuation systems.^{7,18-22} UGa_3 does not behave as a spin fluctuation system, but is an itinerant $5f$ electron antiferromagnet. In fitting the transient change in reflectivity for UAl_3 and USn_3 , we needed a two-exponential decay function below T_{sf} , which points to the presence of

two relaxation channels below T_{sf} . This arises from the hybridization between f electrons and conduction electrons below T_{sf} . This shows that the ultrafast pump probe technique is sensitive to c - f hybridization in f -electron systems. Our T_{sf} is consistent with that obtained from resistivity and susceptibility measurements. We were also able to fit the temperature dependence of the relaxation amplitude and time using the RT model. For UGa_3 , the relaxation time diverges as the temperature approaches the Néel temperature T_N , corresponding to the formation of a spin density wave (SDW) gap near the Fermi level.

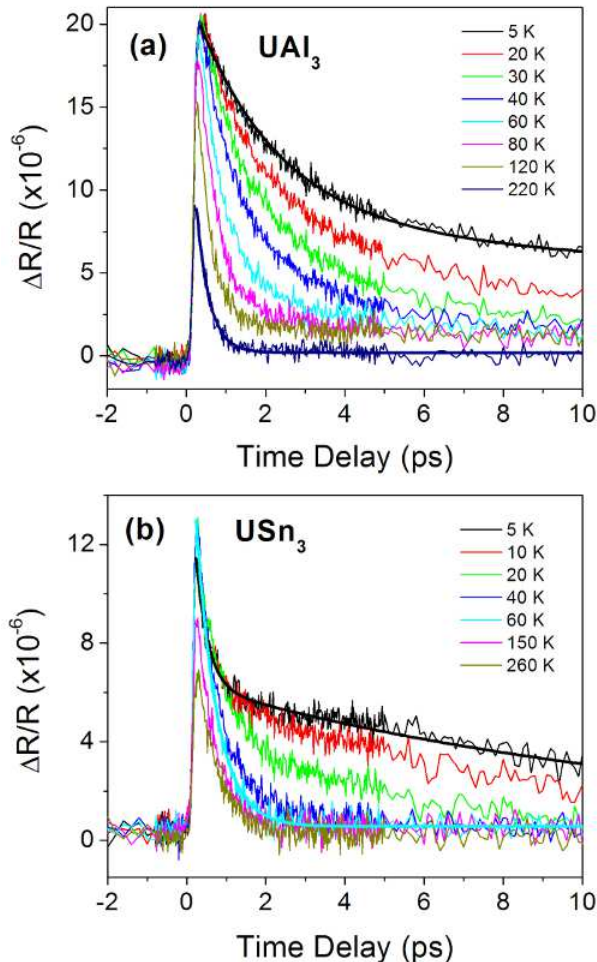


FIG. 1: Transient reflection $\Delta R/R$ versus pump-probe time delay at different temperatures for (a) UAl_3 , and (b) USn_3 . Thick solid curves denote exponential fits of data.

II. EXPERIMENTAL SETUP

In our pump-probe experimental setup in reflectance geometry, a Ti:sapphire laser producing sub-100 fs pulses at ≈ 800 nm (1.55 eV) was used as a source of both pump and probe pulses. The pump and probe pulses were cross

polarized. The pump spot diameter was $60 \mu\text{m}$ and that of probe was $30 \mu\text{m}$. The reflected probe beam was focused onto an avalanche photodiode detector. The photoinduced change in reflectivity ($\Delta R/R$) was measured using lock-in detection. In order to minimize noise, the pump beam was modulated at 100 kHz with an acousto-optical modulator. The experiments were performed with an average pump power of 2 mW, giving a pump fluence of $\sim 1 \mu\text{J}/\text{cm}^2$. The probe intensity was approximately ten times lower. Data were taken from 10 K to 300 K. The experiments were performed on single crystals of UX_3 ($X = \text{Al}, \text{Ga}, \text{Sn}$) grown using standard flux technique, with X used as the flux in each case.²²

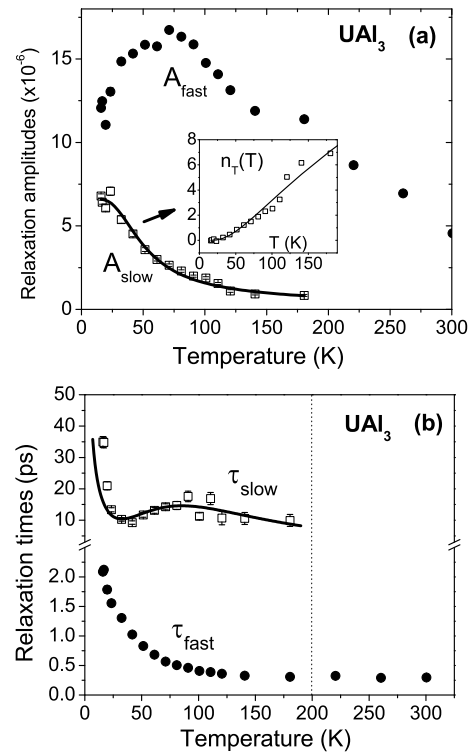


FIG. 2: Temperature dependence of (a) amplitudes and (b) relaxation times for UAl_3 . Solid lines are fits to the RT model of the slow component.

III. UAl_3 AND USn_3

In Fig. 1 we show the $\Delta R/R$ at different temperatures for (a) UAl_3 and (b) USn_3 , as a function of the time delay between the pump and probe pulses. In both UAl_3 and USn_3 , only a fast relaxation of ~ 500 fs, which is typical of regular metals, is observed at high temperatures. At low temperatures, an additional slow, positive picosecond relaxation is observed. Data at low temperatures are fit-

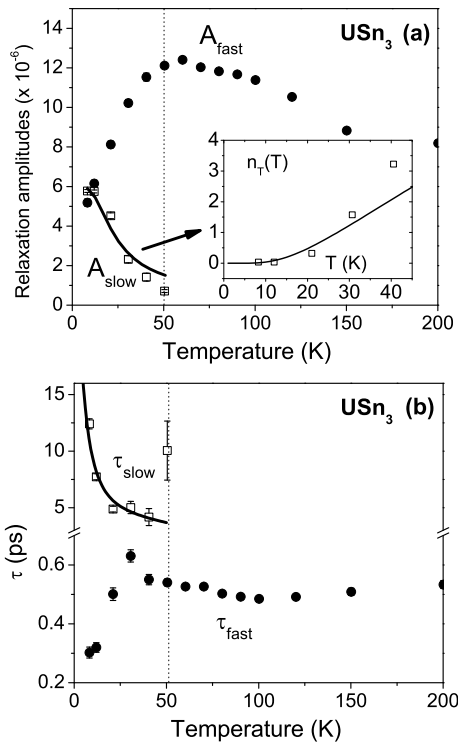


FIG. 3: Temperature dependence of (a) amplitude and (b) relaxation time for USn_3 . Solid lines are fits to the RT model of the slow component.

ted to the two-exponential decay function $\Delta R/R(t) = A_{fast}(T) \exp(-t/\tau_{fast}) + A_{slow}(T) \exp(-t/\tau_{slow})$. This change from one- to two-exponential decay occurs at a particular crossover temperature — ~ 200 K for UAl_3 and ~ 50 K for USn_3 , suggestive of two relaxation channels below this crossover temperature. These crossover temperatures are of the order of the spin fluctuation temperatures T_{sf} obtained in these compounds from temperature-dependent electrical resistivity and magnetic susceptibility measurements (~ 150 K for UAl_3 ^{6,23} and ~ 50 K for USn_3 ^{6,24,25}) We thus associate this crossover temperature to the spin fluctuation temperature T_{sf} .

To understand the different characteristic temperatures in UAl_3 and USn_3 , we have also performed band structure calculations in the framework of the density functional theory, by using the WIEN2k linearized augmented plane wave method.²⁶ A generalized gradient approximation²⁷ was used to treat exchange and correlation. Spin-orbit coupling was included in a second-variational way. The obtained U partial 5f density of states, as shown in Fig. 4, indicates a narrower peak width near the Fermi energy, in USn_3 as compared with UAl_3 . In addition, one can see that the splitting between the two major peaks is smaller in USn_3 than in UAl_3 . In

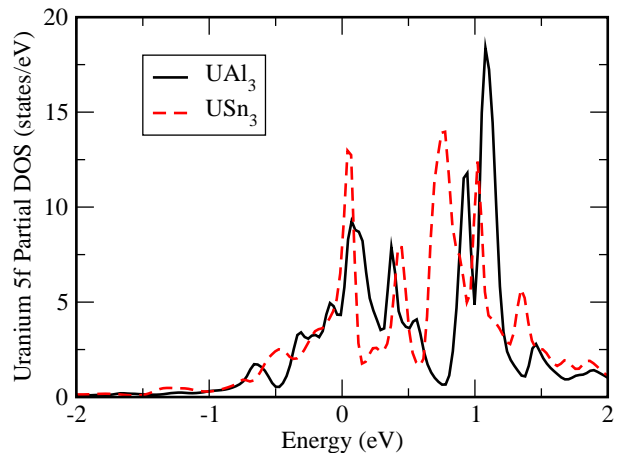


FIG. 4: Total DOS calculated from the LAPW method for UAl_3 and USn_3 , in the magnetic unit cell, in the energy range $(-2,2)$ eV. Note the narrower peak width near the Fermi energy ($E=0$) in USn_3 compared to UAl_3 .

view of the fact that the spin-orbit coupling is quite local to the U atoms, one would expect the same effect on both USn_3 and UAl_3 . A reasonable explanation for this difference is a smaller hybridization gap in USn_3 compared to UAl_3 , due to the weakening of the hybridization in USn_3 — a result of the lattice expansion ($a=4.626$ Å in USn_3 versus $a=4.264$ Å in UAl_3).²³ Though conventional band structure calculations underestimate the correlation effect, the trend of smaller coherence energy scale in USn_3 than in UAl_3 should be robust, as has recently been exemplified in other isostructural actinide compounds.²⁸

In this context, the two-exponential behavior at low temperature can be explained by the c - f hybridization occurring below T_{sf} . Below T_{sf} , the interaction of partially-filled f shell electrons with conduction electrons lead to the formation of heavy quasiparticles.²⁹ As the f -electrons are localized above T_{sf} , relaxation occurs through phonon channel only. Hence only a single exponential decay is expected above T_{sf} . When $T < T_{sf}$, the spin fluctuation channel opens up due to hybridization. Electrons now relax via *both* phonon and spin fluctuation channels resulting in a two-exponential decay behavior. Also, a higher T_{sf} value in UAl_3 compared to USn_3 points to a stronger c - f hybridization, which is expected, as c - f hybridization tends to decrease as the size of the non- f atom increases,^{3,30} which causes the lattice expansion as we discussed above.

The hybridization between the conduction band and the localized f -levels also results in the formation of a narrow gap in the density of states near the Fermi level, called the hybridization gap. The presence of this gap causes a bottleneck in quasiparticle relaxation, resulting in a divergence of the relaxation time at low temperatures. The temperature dependence of the relaxation amplitude and relaxation time can be quantitatively explained by the Rothwarf-Taylor (RT) model. It is a phenomenological model that was used to describe the re-

relaxation of photoexcited superconductors,^{31,32} itinerant antiferromagnets^{14,15} and heavy-fermion metals,¹⁷ where the presence of a gap in the electronic density of states gives rise to a relaxation bottleneck for carrier relaxation. In heavy fermions, after the initial photo-excitation by a pump pulse, the subsequent fast relaxation due to electron-electron scattering results in excess densities of electron-hole pairs (EHPs) and high-frequency phonons (HFPs). When an EHP with energy $\geq \Delta$ (Δ = hybridization gap) recombines, a HFP is created. The HFPs released in the EHP recombination are trapped within the excited volume and can re-excite EHPs; hence they act as a bottleneck for EHP recombination, and recovery is governed by the decay of the HFP population. The evolution of EHP and HFP populations is described by a set of two coupled nonlinear differential equations.

The results of the RT model are as follows:^{17,33} from the amplitude $A(T)$, one obtains the density of thermally excited EHPs n_T via the relation

$$n_T(T) \propto \mathcal{A}(T)^{-1} - 1 \quad (1)$$

where $\mathcal{A}(T)$ is the normalized amplitude ($\mathcal{A}(T) = A(T)/A(T \rightarrow 0)$). Then we fit the experimental $n_T(T)$ to the expression¹⁷

$$n_T(T) \propto \sqrt{T} \exp(-\Delta/T), \quad (2)$$

where the hybridization gap Δ is temperature independent (or very weakly temperature dependent) and can be obtained from the fitting. Moreover, for a constant pump intensity, the temperature-dependence of n_T also governs the temperature-dependence of τ^{-1} , given by

$$\tau^{-1}(T) = \Gamma[\delta(\beta n_T + 1)^{-1} + 2n_T](\Delta + \alpha T \Delta^4) \quad (3)$$

where Γ , δ , β and α are T -independent fitting parameters.

Since, below T_{sf} , the second relaxation component appears, we attribute it to relaxation across the hybridization gap, and use the RT model to fit the its amplitude and relaxation time below T_{sf} in UAl_3 and USn_3 . The inset of Fig. 2(a) shows $n_T(T)$ obtained from $A_{slow}(T)$ using Eq. (1), with the solid line being the fit to Eq. (2), with the fitting parameter $\Delta \approx (230 \pm 10)$ K. The fitted values of $n_T(T)$ are then inserted into Eq. (3) to fit the experimental values of $\tau_{slow}(T)$, shown in Fig. 2(b). Similar fits are also done for USn_3 , as shown in Fig. 3, yielding $\Delta \approx (90 \pm 20)$ K. The good fits show that the slow relaxation component in both UAl_3 and USn_3 can be described by assuming EHPs relaxing across the hybridization gap near the Fermi surface. More interestingly, the extracted hybridization gap in UAl_3 is larger than in USn_3 , in qualitative agreement with the band structure results. This comparison of hybridization gap is also consistent with that of spin fluctuation energy scale T_{sf} discussed above. Our results show that the ultrafast pump-probe technique is sensitive to the hybridization of f -electron orbitals with the conduction electron orbitals.

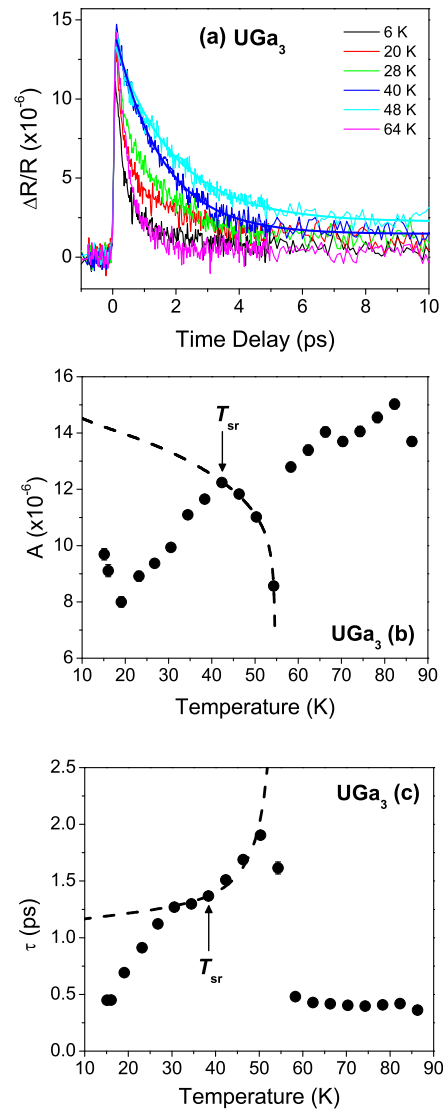


FIG. 5: (a) Photoinduced change in reflectivity $\Delta R/R$ versus pump-probe time delay at different temperatures of UGa_3 . Thick blue (cyan) curves denote one-exponential fits of data at $T=40$ K (48 K). Temperature dependence of (b) amplitude and (c) relaxation time for UGa_3 obtained from one-exponential fits, with dashed lines in (b) and (c) being fits to the RT model from 40 K to T_N .

IV. UGa_3

We now turn to the relaxation dynamics of UGa_3 . UGa_3 is not a spin fluctuation system — it is a SDW system with Néel temperature $T_N=65$ K. It is a moderate heavy fermion with Sommerfeld coefficient $52 \text{ mJ/K}^2 \cdot \text{mol}$,³⁴ and is reported to follow a modified Curie-Weiss law behavior³⁵ with $T^*=2080$ K which is in-

dicative of strong hybridization in this compound. The $5f$ electrons in UGa_3 can be considered itinerant because of the large hybridization of $5f$ orbitals with conduction electron orbitals. The photoinduced change in reflectivity, as shown in Fig. 5(a), can be fitted with a single exponential decay $\Delta R/R(t) = A(T) \exp(-t/\tau)$. The extracted relaxation amplitude $A(T)$ and time $\tau(T)$ are shown in Fig. 5(b) and Fig. 5(c), respectively. Upon entering the SDW phase, $A(T)$ increases with decreasing temperature. However, instead of monotonically increasing as in UAl_3 and USn_3 , $A(T)$ now attains a maximum at ~ 40 K and starts decreasing with decreasing temperature (see Fig. 5(b)). Concurrently, τ exhibits a quasi-divergence at T_N , consistent with that observed in itinerant antiferromagnets UNiGa_5 and UPtGa_5 , where the opening up of the SDW gap causes a bottleneck in quasiparticle relaxation.^{14,15} In contrast to UNiGa_5 and UPtGa_5 , however, where τ increases with decreasing temperature at low temperatures, τ in UGa_3 shows a (1) shoulder (or change in curvature) at 40 K, and (2) decrease with decreasing temperature. An anomaly at a spin-reorientation temperature $T_{sr}=40$ K has been reported in other measurements of UGa_3 , whether in the presence of a magnetic field (nuclear magnetic resonance, neutron scattering, magnetic susceptibility),^{36–40} or in the absence of a magnetic field (thermal conductivity and neutron scattering).^{36,37} This anomaly has been associated with a reorientation of the ordered magnetic moments, which induces strong modifications of the uranium $5f$ orbitals.³⁹ The fact that the transition is observed in the absence of magnetic field is an indication that the bump we see at 40 K in our pump probe measurement is not an artifact, but corresponds to the moment reorientation as has been reported in other measurements mentioned above.

We use the model proposed by Kabanov *et al.*⁴¹ to analyze the temperature dependence of A . The temperature-dependence of the relaxation amplitude in the SDW state for an isotropic temperature-dependent gap $\Delta_{SDW}(T)$ is given by (writing $\Delta_{SDW}(T)$ as $\Delta(T)$)

$$A(T) = \frac{\epsilon_I / (\Delta(T) + k_B T / 2)}{1 + \zeta \sqrt{\frac{2k_B T}{\pi \Delta(T)}} \exp[-\Delta(T) / k_B T]}, \quad (4)$$

where ϵ_I the pump laser intensity per unit cell, ζ is a constant, and $\Delta(T)$ obeys a weak-coupling BCS temperature dependence. The above expression for $A(T)$ describes a reduction in the photoexcited quasiparticle density with increase in temperature, due to the decrease in gap energy and corresponding enhanced phonon emission dur-

ing the initial relaxation. A good fit between the experimental $A(T)$ and Eq. (4) can only be made from T_N down to ~ 40 K, where $T_N=55$ K is a fitting parameter. In the SDW state ($T < T_N$), the temperature-dependence of τ can be obtained from Eq. (3), but can be written in the alternative form (writing $\Delta_{SDW}(T)$ as $\Delta(T)$)¹³

$$\tau^{-1}(T) = \Gamma \{ \delta A(T) + \eta \sqrt{\Delta(T)T} \exp[-\Delta(T)/T] \} \times [\Delta(T) + \alpha T \Delta(T)^4]. \quad (5)$$

The fit of $\tau(T)$ to Eq. (5) is shown in Fig. 5(c). Once again, a good fit is obtained only from T_N to ~ 30 K, close to T_{sr} . Below T_{sr} , the fit deviates from the experimental data, consistent with the existence of another transition at T_{sr} .

V. CONCLUSION

We have performed time-resolved photoinduced change in reflectivity measurements on three isostructural uranium compounds — UAl_3 , UGa_3 and USn_3 . The values of T_{sf} , a measure of the degree of hybridization, in UAl_3 and USn_3 , are consistent with data from other measurements. Our fit of the slow component to the Rothwarf-Taylor model shows that the slow component can be described by assuming electron-hole pairs relaxing across the hybridization gap. We have thus shown the pump probe technique to be sensitive to c - f hybridization. Our data on UGa_3 is consistent with the formation of a SDW gap at $T_N=60$ K, and a reorientation of magnetic moments at $T_{sr}=40$ K.

VI. ACKNOWLEDGEMENTS

E.E.M.C. acknowledges support from G. T. Seaborg Postdoctoral Fellowship, the Singapore Ministry of Education Academic Research Fund Tier 2 (ARC23/08), as well as the National Research Foundation Competitive Research Programme (NRF-CRP4-2008-04). Work at Los Alamos was supported by the U.S. DOE at LANL under Contract No. DE-AC52-06NA25396, the U.S. DOE Office of Basic Energy Sciences, and the LDRD Program at LANL. The electronic structure calculations were performed on a computer cluster at the Center for Integrated Nanotechnologies, a U.S. DOE Office of Basic Energy Sciences user facility.

¹ J. M. Fournier and R. Troć, *Handbook on the Physics and Chemistry of the Actinides*, vol. 2 (North-Holland, Amsterdam, 1985).

² H. H. Hill, in *Plutonium and other Actinides*, edited by

W. N. Miner (Nuclear Materials Sciences, AIME, New York, 1970), vol. 17, pp. 2–17.

³ D. D. Koelling, B. D. Dunlap, and G. W. Crabtree, *Phys. Rev. B* **31**, 4966 (1985).

- ⁴ H. R. Ott, F. Hulliger, H. Rudigier, and Z. Fisk, Phys. Rev. B **31**, 1329 (1985).
- ⁵ A. J. Arko, M. B. Brodsky, and W. J. Nellis, Phys. Rev. B **5**, 4564 (1972).
- ⁶ R. Jullien and B. Coqblin, J. Low Temp. Phys. **22**, 437 (1976).
- ⁷ K. H. J. Buschow and H. J. van Daal, AIP Conference Proceedings **5**, 1464 (1972).
- ⁸ R. Jullien, M. T. Béal-Monod, and B. Coqblin, Phys. Rev. Lett. **30**, 1057 (1973).
- ⁹ R. Jullien, M. T. Béal-Monod, and B. Coqblin, Phys. Rev. B **9**, 1441 (1974).
- ¹⁰ C. L. Lin, L. W. Zhou, J. E. Crow, and R. P. Guertin, J. Appl. Phys. **57**, 3146 (1985).
- ¹¹ T. Yuen, Y. Gao, I. Perez, and J. E. Crow, J. Appl. Phys. **67**, 4827 (1990).
- ¹² E. E. M. Chia, J.-X. Zhu, D. Talbayev, R. D. Averitt, A. J. Taylor, K. H. Oh, I. S. Jo, and S. I. Lee, Phys. Rev. Lett. **99**, 147008 (2007).
- ¹³ S. K. Nair, X. Q. Zou, E. E. M. Chia, J.-X. Zhu, C. Panagopoulos, S. Ishida, and S. Uchida, Phys. Rev. B **82**, 212503 (2010).
- ¹⁴ E. E. M. Chia, J.-X. Zhu, H. J. Lee, N. Hur, N. O. Moreno, E. D. Bauer, T. Durakiewicz, R. D. Averitt, J. L. Sarrao, and A. J. Taylor, Phys. Rev. B **74**, 140409 (2006).
- ¹⁵ E. E. M. Chia, J.-X. Zhu, D. Talbayev, H. J. Lee, N. Hur, N. O. Moreno, R. D. Averitt, J. L. Sarrao, and A. J. Taylor, Phys. Rev. B **84**, 174412 (2011).
- ¹⁶ D. Talbayev, K. S. Burch, E. E. M. Chia, S. A. Trugman, J.-X. Zhu, E. D. Bauer, J. A. Kennison, J. N. Mitchell, J. Thompson, J. L. Sarrao, et al., Phys. Rev. Lett. **104**, 227002 (2010).
- ¹⁷ J. Demsar, J. L. Sarrao, and A. J. Taylor, J. Phys.: Condens. Matter **18**, R281 (2006).
- ¹⁸ M. H. Van Maaren, H. J. Van Daal, K. H. J. Buschow, and C. J. Schinkel, Solid State Commun. **14**, 145 (1974).
- ¹⁹ I. Lupsa, P. Lucaci, and E. Burzo, J. Alloys Compd. **204**, 247 (1994).
- ²⁰ I. Lupsa, E. Burzo, and P. Lucaci, J. Magn. Magn. Mater. **157**, 696 (1996).
- ²¹ M. R. Norman, S. D. Bader, and H. A. Kierstead, Phys. Rev. B **33**, 8035 (1986).
- ²² A. L. Cornelius, A. J. Arko, J. L. Sarrao, J. D. Thompson, M. F. Hundley, C. H. Booth, N. Harrison, and P. M. Oppeneer, Phys. Rev. B **59**, 14473 (1999).
- ²³ D. Aoki, N. Watanabe, Y. Inada, R. Settai, K. Sugiyama, H. Harima, T. Inoue, K. Kindo, E. Yamamoto, Y. Haga, et al., J. Phys. Soc. Jpn. **69**, 2609 (2000).
- ²⁴ M. Loewenhaupt and C. K. Loong, Phys. Rev. B **41**, 9294 (1990).
- ²⁵ K. Sugiyama, T. Iizuka, et al., J. Phys. Soc. Jpn. **71**, 326 (2002), ISSN 0031-9015.
- ²⁶ P. Blaha, K. Schwarz, G. K. H. Madsen, D. Kvasnicka, and J. Luitz, *WIEN2k, An Augmented Plane Wave Plus Local Orbitals Program for Calculating Crystal Properties* (Vienna University of Technology, Austria, 2001).
- ²⁷ J. P. Perdew, K. Burke, and M. Ernzerhof, Phys. Rev. Lett. **77**, 3865 (1996).
- ²⁸ J.-X. Zhu, P. H. Tobash, E. D. Bauer, F. Ronning, B. L. Scott, K. Haule, G. Kotliar, R. C. Albers, and J. M. Wills, Europhys. Lett. **97**, 57001 (2012).
- ²⁹ A. I. Lobad, A. J. Taylor, J. L. Sarrao, and S. A. Trugman, in *Quantum Electronics and Laser Science Conference, 2000. (QELS 2000). Technical Digest* (2000), pp. 159 – 160.
- ³⁰ A. J. Arko and D. D. Koelling, Phys. Rev. B **17**, 3104 (1978).
- ³¹ A. Rothwarf and B. N. Taylor, Phys. Rev. Lett. **19**, 27 (1967).
- ³² J. Demsar, R. D. Averitt, A. J. Taylor, V. V. Kabanov, W. N. Kang, H. J. Kim, E. M. Choi, and S. I. Lee, Phys. Rev. Lett. **91**, 267002 (2003).
- ³³ V. V. Kabanov, J. Demsar, and D. Mihailovic, Phys. Rev. Lett. **95**, 147002 (2005).
- ³⁴ M. Biasini, J. Ruzs, G. Ferro, and A. Czopnik, Acta Phys. Pol. A **107**, 554 (2005).
- ³⁵ L. W. Zhou, C. S. Jee, C. L. Lin, J. E. Crow, S. Bloom, and R. P. Guertin, J. Appl. Phys. **61**, 3377 (1987).
- ³⁶ D. Kaczorowski, P. W. Klamut, A. Czopnik, and A. Jeżowski, J. Magn. Magn. Mater. **177**, 41 (1998).
- ³⁷ P. Dervenagas, D. Kaczorowski, F. Bourdarot, P. Burlet, A. Czopnik, and G. H. Lander, Physica B **269**, 368 (1999).
- ³⁸ S. Kambe, H. Kato, H. Sakai, R. E. Walstedt, Y. Haga, D. Aoki, and Y. Ônuki, Physica B **312**, 902 (2002).
- ³⁹ S. Kambe, H. Kato, H. Sakai, Y. Tokunaga, R. E. Walstedt, Y. Haga, H. Yasuoka, and D. Aoki, Physica B **329**, 614 (2003).
- ⁴⁰ S. Kambe, R. E. Walstedt, H. Sakai, Y. Tokunaga, T. D. Matsuda, Y. Haga, and Y. Ônuki, Phys. Rev. B **72**, 184437 (2005).
- ⁴¹ V. V. Kabanov, J. Demsar, B. Podobnik, and D. Mihailovic, Phys. Rev. B **59**, 1497 (1999).